NUCLEAR SCIENCE AND TECHNIQUES **26**, 010601 (2015)

Minimizing torque ripple in a brushless DC motor with fuzzy logic: applied to control rod driving mechanism of MNSR*

Mohammad Divandari,[1,†] Mehdi Hashemi-Tilehnoee,[1] Bahram Asgari-Ziarati,[1] Mohammadreza Hosseinkhah,[1] and Khashayar Sabagh[2]

[1] *Department of Electrical Engineering, Aliabad Katoul branch, Islamic Azad University, Aliabad Katoul 93451-49417, Iran*

[2] *Department of Mechanical Engineering, Babol Noshirvani University of Technology, Babol 71167-47148, Iran*

(Received August 11, 2014; accepted in revised form November 1, 2014; published online February 20, 2015)

A permanent magnet BLDC (brushless direct current) motor is used to move the control rod of a miniature neutron source reactor (MNSR). The BLDC motor drive is modeled using MATLAB/SIMULINK. Two main parts of the modeling are the inverter switching and the current control. Current control with chopping used to minimize the torque ripple of the MNSR control rod drive. Fuzzy logic current control together with soft chopping control shows the best response of all the three strategies. The prototype drive mechanism has an ATmega32 controller and power MOSFET switches. The simulation results are compared with experimental drive mechanism.

Keywords: Torque ripple, BLDC motor, Fuzzy logic, Control rod, MNSR

DOI: 10.13538/j.1001-8042/nst.26.010601

I. INTRODUCTION

The permanent magnet brushless direct current (BLDC) motor has been widely used in industrial applications of variable speed drives. The BLDC motor produces torque from the interaction of magnetic flux of the rotor magnets and the current carrying stator conductors of the stator core assembly. Its benefits include high power density, high efficiency, low maintenance, high reliability, simplicity, lower price, and fast dynamic response.

Stator current commutation torque ripples, occurring due to the loss of ideal phase current commutation and the methods to minimize ripples, have been reported in literatures. Ashabani *et al.* reduced torque ripple of BLDC motor by control of the DC link voltage during the commutation time [1]. The intelligence method was the basis of their research, where the magnitude of voltage and commutation time were estimated by a neural network and optimized with particle swarm optimization (PSO) algorithm.

In 2011 and 2014, the brushless linear DC motor was proposed to move the nuclear reactor control rod-assemblies as primary and auxiliary driving motor, respectively [2, 3]. In this study, the BLDC motor was employed to move the only control rod of a miniature neutron source reactor (MNSR). Torque ripple of the BLDC motor minimizes with fuzzy logic to satisfy the requirements of fast response and precision movement of the control rod.

* Supported by Research Contract of the Islamic Azad University's Aliabad Katoul branch

† Corresponding author, mohammad.divandari@gmail.com

II. REACTOR DESCRIPTION

The MNSR developed by the Chinese Institute of Atomic Energy, is a compact research reactor based on the Canadian SLOWPOKE reactor design. It is of a low power tank-in-pool type and uses highly enriched uranium as fuel, light water as moderator and coolant, and metallic beryllium plates as reflector [3]. The core consists of the fuel cage, one central cadmium absorber with stainless steel cladding control rod, fuel pins (fuel rods), dummy rods, and tie rods, with the generated heat removed through natural circulation [4].

A. Reactor description

The control rod drive mechanism (CRDM) is driven by a servo motor, type SDE-45 through a mechanical gear system. The servo motor ensures position control of the control rod, and hence stability of the neutron-flux. The CRDM assembly is mounted on top of the reactor vessel, about 0.6 m above the volume of reactor pool water. The pool top is covered with a Perspex material to protect the pool water from environmental contamination and to reduce evaporation. Although most of the materials in the control rod drive mechanism assembly are made of stainless steel, the servo motor contains corrodible materials [5, 6].

In 2014, an electromagnetic levitation system together with synchronous motor was used to navigate the control rod. The control system was programmed in MATLAB through the open-loop system, closed-loop with state feedback, and closed-loop with state feedback integral tracking. The results from the prototype system showed that the proposed method was useful in such a sensitive drive mechanism [4].

III. MODELING OF BLDC

The BLDC motor back electromotive force (back-EMF) induced in stator windings has a trapezoidal shape. In this study, due to high efficiency, cost effective control, optimum number of power electronic devices (number of MOSFETs), and low torque ripple, the three phases of BLDC motor have been used. Fig. 1 shows the cross section of the three-phase BLDC motor construction.

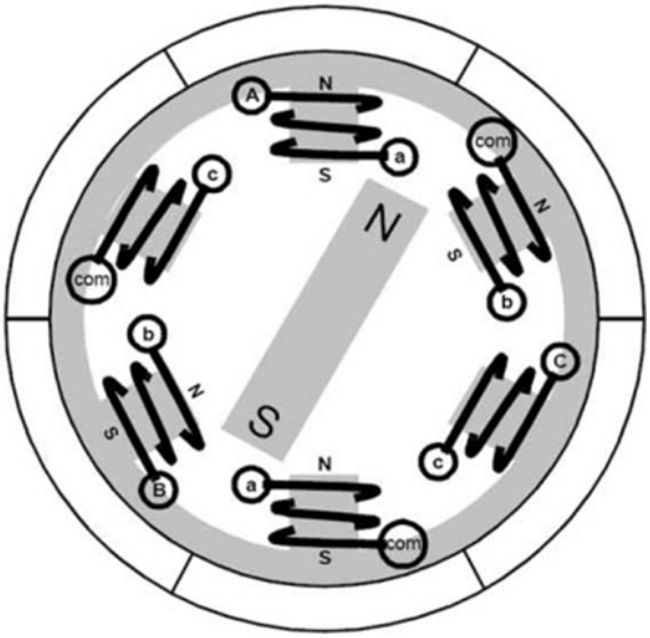

Fig. 1. Cross section of the three-phase BLDC motor construction.

The BLDC drive modeling is implemented based on the following steps:

- The phase currents and position are measured;
- Differential equations of the BLDC consist of speed, position, and the current of phases a and b;
- Trapezoidal back-EMF of BLDC drive simulated using a look-up table;
- By means of torque ripple minimization an inverter with soft chopping has been used;
- The current control unit provides a DC voltage level of the inverter.

Figure 2 shows the schematic of the BLDC drive modeling.

A. BLDC differential equations

Fundamental of differential equations in BLDC motor can be written as (refer to Fig. 2 for the variants) [7]

$$v_{ab} = Ri_{ab} + R\mathrm{d}i_{ab}/\mathrm{d}t + E_{ab}, \tag{1}$$

$$v_{bc} = Ri_{bc} + R\mathrm{d}i_{bc}/\mathrm{d}t + E_{bc}, \tag{2}$$

$$v_{ca} = Ri_{ca} + R\mathrm{d}i_{ca}/\mathrm{d}t + E_{ca}, \tag{3}$$

$$i_{ab} = i_a - i_b, \quad E_{ab} = e_a - e_b, \tag{4}$$

$$i_{bc} = i_b - i_c, \quad E_{bc} = e_b - e_c, \tag{5}$$

$$i_{ca} = i_c - i_a, \quad E_{ca} = e_c - e_a, \tag{6}$$

$$i_a + i_b + i_c = 0, \tag{7}$$

where v_{ab}, v_{bc} and v_{ca} are line-to-line voltage in the three phases a, b and c; i_{ab}, i_{bc} and i_{ca} are line-to-line current in the three phases; i_a, i_b and i_c are current of the three phases; E_{ab}, E_{bc} and E_{ca} are line-to-line back-EMF in the three phases; e_a, e_b and e_c are voltage of the three phases; R is the phase resistance (Ω).

The back-EMF for three-phases are [6]

$$e_a = k_{e\omega}K(\theta), \tag{8}$$

$$e_b = k_{e\omega}K(\theta - 120^\circ), \tag{9}$$

$$e_c = k_{e\omega}K(\theta - 240^\circ), \tag{10}$$

$$K(\theta) = \begin{cases} 1 & 0 \le \theta < 120^\circ \\ 1 - 6(\theta - 120^\circ)/\pi & 120^\circ \le \theta < 180^\circ \\ -1 & 180^\circ \le \theta < 300^\circ \\ 1 - 6(\theta - 300^\circ)/\pi & 300^\circ \le \theta < 360^\circ \end{cases}, \tag{11}$$

$$k_{e\omega} = k_e\omega_m/2, \tag{12}$$

where, k_e is back-EMF constant (V s/rad), ω is angular velocity (rad/s), θ is the angular displacement (radian) and $K(\theta)$ is trapezoidal waveform of the back-EMF. The electromechanical torque can be expressed as [7]

$$T_e - T_L = k_f\omega_m + J\mathrm{d}\omega_m/\mathrm{d}t, \tag{13}$$

where, T_e is electromagnetic torque (N m), T_L is load torque (N m), k_f is motor friction constant (N s/rad) and J is rotor inertia (kg m^2). The BLDC torque is a function of the current and the back-EMF

$$T_e = k_t[K(\theta)i_a + K(\theta - 120^\circ)i_b + K(\theta - 240^\circ)i_c]/2, \tag{14}$$

where k_t is torque constant (N m/A). From Eqs. (2) and (7), one has

$$v_{bc} = R(i_a + 2i_b) + L\mathrm{d}(i_a + 2i_b)\mathrm{d}t + E_{bc}, \tag{15}$$

where L is phase inductance (H). According to Eqs. (1), (2) and (15), the BLDC motor differential equations for three-phase can be reduced to two-phase as below

$$\mathrm{d}i_a/\mathrm{d}t = -Ri_a/L + 2(v_{ab} - E_{ab})/(3L) + (v_{bc} - E_{bc})/(3L), \tag{16}$$

$$\mathrm{d}i_b/\mathrm{d}t = -Ri_b/L - (v_{ab} - E_{ab})/(3L) + (v_{bc} - E_{bc})/(3L), \tag{17}$$

Equation (13) can be simplified to

$$\mathrm{d}\omega_m/\mathrm{d}t = (T_e - T_L - k_f\omega_m)/J, \tag{18}$$

where

$$\mathrm{d}\theta_m/\mathrm{d}t = \omega_m. \tag{19}$$

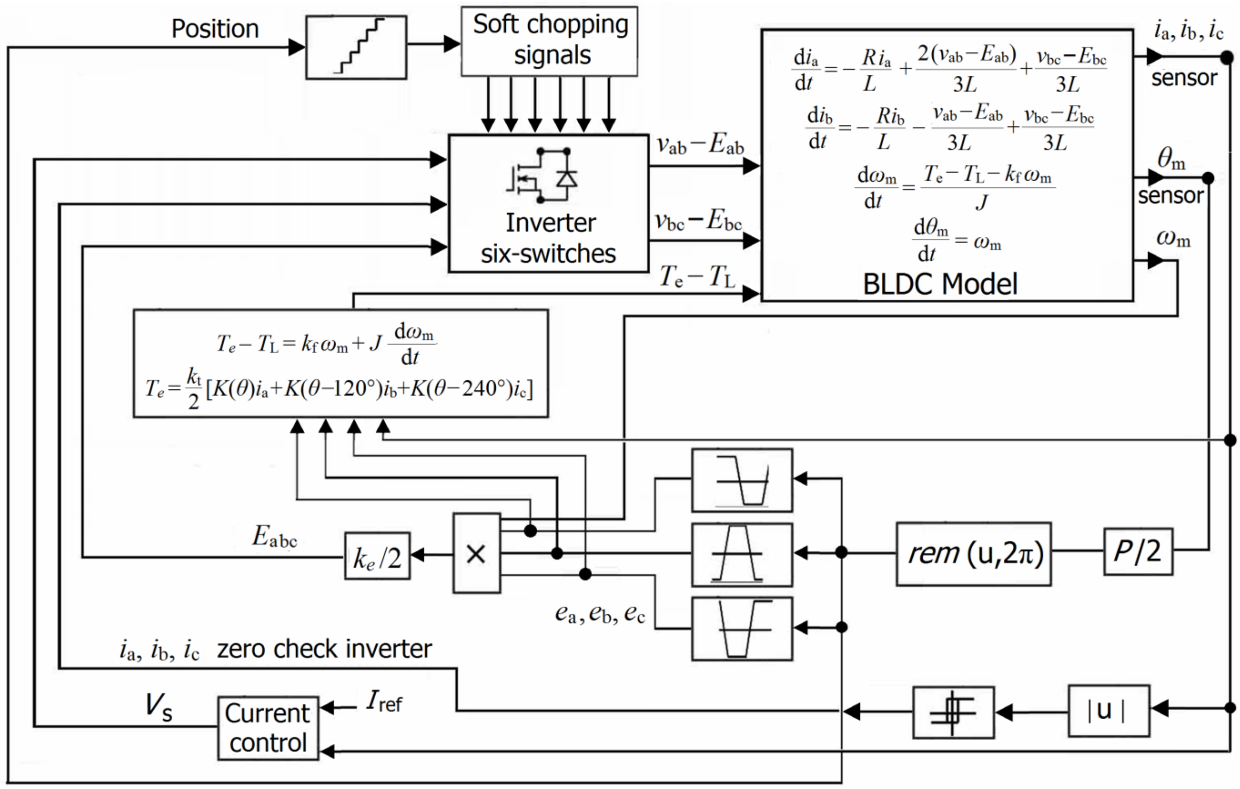

Fig. 2. Schematic of the modeling steps.

B. Inverter of BLDC drive

The BLDC motor drive was actuated by a six-switch inverter as shown in Fig. 3. The switches are metal oxide semiconductor field effect transistor (MOSFET) [7].

In an inverter, the current in active phase was turned on and off by the electronic devices, usually at a high frequency. It is called chopping. Chopping can be done by hard chopping and soft chopping. In hard chopping, the upper and lower switches are driven by the same signal; while in soft chopping, only the upper switch is driven by the chopping signal and the lower switch is left on during the whole interval. The advantage of soft chopping is that it creates less switching losses and current ripple than the hard chopping, hence the minimized torque ripple. Proposed soft chopping circuit is shown in Fig. 4. The inverter voltages in soft chopping mode applied to six-switch inverter are given in Table 1.

C. Current control of BLDC drive

There are two main sources of torque ripple generated by the BLDC drives: chopping in inverter and current control. By means of torque ripple minimization, a new soft chopping control has been presented in this study, and the current control in the BLDC drive via hysteresis current control (HCC) and fuzzy logic current control (FLCC) was investigated.

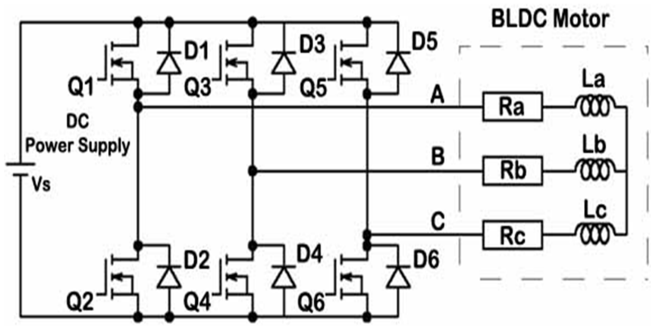

Fig. 3. Schematics of the six-switch inverter.

1. Hysteresis current control

Reviewing researches in the past decade about torque ripple reduction BLDC drive, most authors worked on the torque ripple reduction by HCC. Current control of hysteresis band is a simple and usual current closed-loop control. In HCC, the value of controlled variable is forced to stay within limits (hysteresis band) around a reference value. HCC technique generates switching frequencies when a narrow hysteresis is used, and the wider the hysteresis band is, the larger the ripple is produced. Fig. 5 is the block diagram of HCC. The uncertain switching frequency makes filtering of electromagnetic noise difficult. Moreover, current chattering produces noise in electronic devices and generates high mechanical stress.

TABLE 1. Inverter output voltages in soft chopping

Rotor position	Phase current (A)	$v_{ab} - e_{ab}$	$v_{bc} - e_{bc}$
0°–60°	$i_a \neq 0, i_c \neq 0$	$-e_a + e_b$	$-e_b + e_c$
	$i_a \neq 0, i_c = 0$	$-e_a + e_b$	$0.5(e_a - e_b)$
	$i_a = 0, i_c \neq 0$	$0.5(e_b - e_c)$	$-e_b + e_c$
	$i_a = 0, i_c = 0$	0	0
60°–120°	$i_a \neq 0, i_b \neq 0$	$-V_s - e_a + e_b$	$V_s - e_b + e_c$
	$i_a \neq 0, i_b = 0$	$0.5(-e_a + e_c)$	$0.5(-e_a + e_c)$
	$i_a = 0, i_b \neq 0$	$0.5(-V_s + e_b - e_c)$	$V_s - e_b + e_c$
	$i_a = 0, i_b = 0$	0	0
120°–180°	$i_b \neq 0, i_a \neq 0$	$-e_a + e_b$	$-e_b + e_c$
	$i_b \neq 0, i_a = 0$	$0.5(e_b - e_c$	$-e_b + e_c$
	$i_b = 0, i_a \neq 0$	$0.5(-e_a + e_c$	$0.5(-e_a + e_c$
	$i_b = 0, i_a = 0$	0	0
180°–240°	$i_b \neq 0, i_c \neq 0$	$-e_a + e_b$	$-V_s - e_b + e_c$
	$i_b \neq 0, i_c = 0$	$-e_a + e_b$	$0.5(e_a - e_b$
	$i_b = 0, i_c \neq 0$	$0.5(-V_s - e_a + e_c)$	$0.5(-V_s - e_a + e_c)$
	$i_b = 0, i_c = 0$	0	0
240°–300°	$i_c \neq 0, i_b \neq 0$	$-e_a + e_b$	$-e_b + e_c$
	$i_c \neq 0, i_b = 0$	$0.5(-e_a + e_c)$	$0.5(-e_a + e_c)$
	$i_c = 0, i_b \neq 0$	$-e_a + e_b$	$0.5(e_a - e_b$
	$i_c = 0, i_b = 0$	0	0
300°–360°	$i_c \neq 0, i_a \neq 0$	$V_s - e_a + e_b$	$-e_b + e_c$
	$i_c \neq 0, i_a = 0$	$0.5(e_b - e_c$	$-e_b + e_c$
	$i_c = 0, i_a \neq 0$	$V_s - e_a + e_b$	$0.5(-V_s + e_a - e_b)$
	$i_c = 0, i_a = 0$	0	0

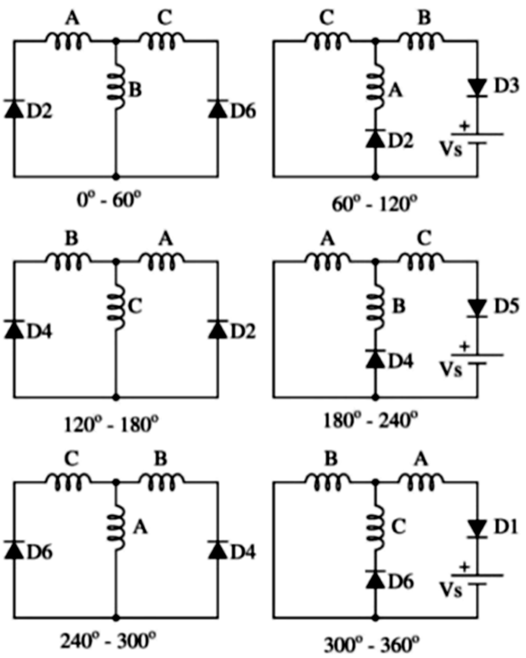

Fig. 4. Circuit configuration during soft chopping.

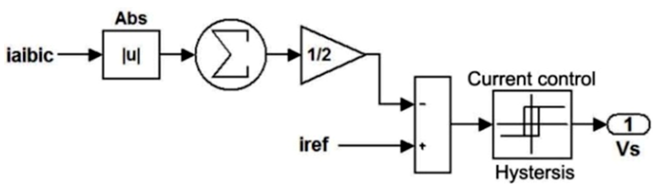

Fig. 5. Block diagram of hysteresis control scheme.

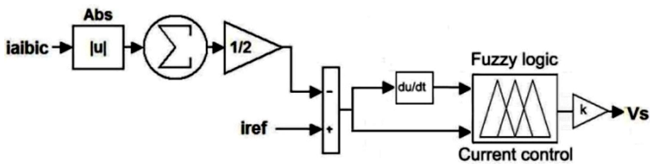

Fig. 6. Block diagram of the current control scheme using fuzzy logic.

2. *Fuzzy logic current control*

The torque ripple of BLDC drive could be minimized by using fuzzy logic current control. The block diagram of FLCC for minimization of torque ripple of BLDC drive is shown in Fig. 6.

Current error is the differential between current reference and root mean square (RMS) of three phase current. In FLCC method, fuzzy rules act on current errors (five member function for −0.5–0.5 A) and current error derivative (seven member function for −0.06–0.06 A/ms) as inputs, and also act on inverter voltage level (five members function for 0–1 V) as output. Fig. 7 shows the fuzzy logic member functions for proposed FLCC.

Table 2 shows the fuzzy logic rules used to reduce the torque ripple.

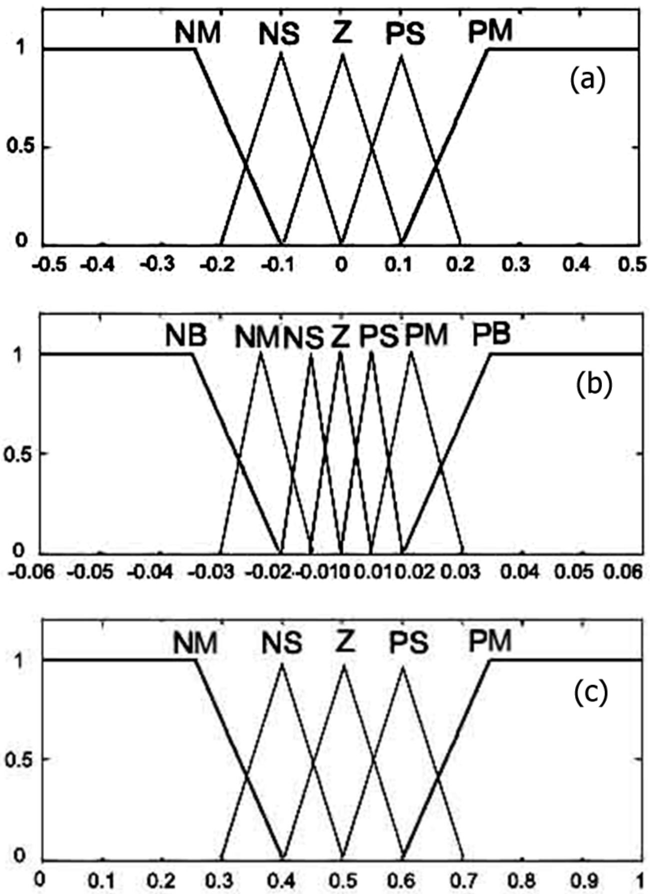

Fig. 7. Fuzzy logic member functions: (a) Current error, (b) Current error derivative, (c) Inverter voltage level.

TABLE 2. Fuzzy rules

Current Error	Current error derivative						
	NB	NM	NS	Z	PS	PM	PB
NM	NS	NM	NM	NM	NM	NM	NM
NS	NS	NS	Z	Z	NS	NS	NM
Z	NM	NS	NS	Z	Z	NS	NS
PS	PM	PM	PS	PS	Z	NS	NS
PM	PM	PM	PM	PM	PM	PM	PS

IV. SIMULATION RESULTS AND DISCUSSION

The proposed BLDC drive which applied to the CRDM of MNSR has been simulated by MATLAB/ SIMULINK. The parameters of the model are listed in table 3.

The BLDC drive has been operated by three cases: a) HCC with hard chopping, b) HCC with soft chopping and c) FLCC with soft chopping. Fig. 8 shows the fast dynamic response of the BLDC motor where the speed of the motor was regulated at 360 RPM. The simulation results of the BLDC drive operation are shown Fig. 9.

From Fig. 9, the total torque of the BLDC motor is affected by current control. The hard chopping control has a good response to HCC rather than soft chopping control with HCC.

TABLE 3. Drive Parameters

Parameters	Value
Number of poles	2
Nominal Power (W)	1.2
Nominal voltage (V)	6
No load speed (RPM)	8000
Terminal resistance phase to phase (Ω)	12.50
Terminal inductance phase to phase (H)	0.091×10^{-3}
No load current (A)	0.5
Back-EMF constant (V s/rad)	1.05×10^{-3}
Torque constant (N m A)	1.05×10^{-3}
Rotor inertia (kg m^2)	0.005×10^{-7}
Friction constant (N s/rad)	1.38×10^{-8}
MNSR control rod mass (g)	50
Control rod length (mm)	230
Control rod speed limit (cm/s)	1.06
Gearbox ratio	1/22
Pulley diameter (cm)	10
MOSFET model of power switches	IRF840
Micro-controller	ATmega32

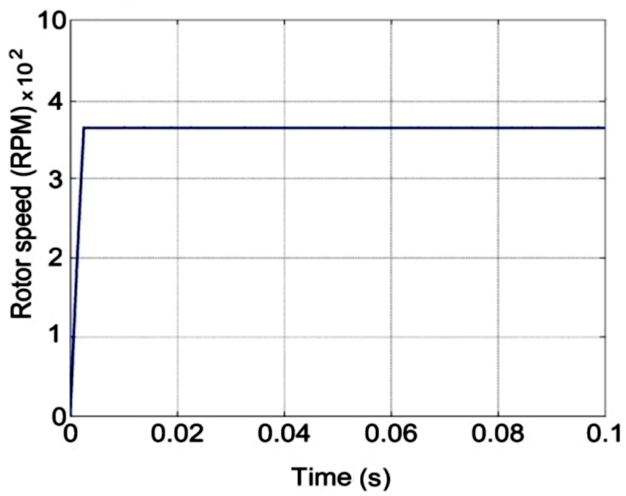

Fig. 8. (Color online) The rotor speed of BLDC motor.

However, the best performance can be obtained using soft chopping with FLCC. This torque ripple reduction technique can be used in such a precision movement of the MNSR control rod drive. A prototype of the optimized drive mechanism with BLDC motor is shown in Fig. 10. This setup includes the BLDC motor, drive, gearbox, and the moving rod. The drive consists of the three parts; power switches (6 MOSFETs), micro-controller, and interface circuits.

V. CONCLUSION

The BLDC motor drive mechanism has been investigated to be used in a research reactor CRDM. The MATLAB/SIMULINK was used to simulate the three understudy cases: HCC with hard chopping, HCC with soft chop-

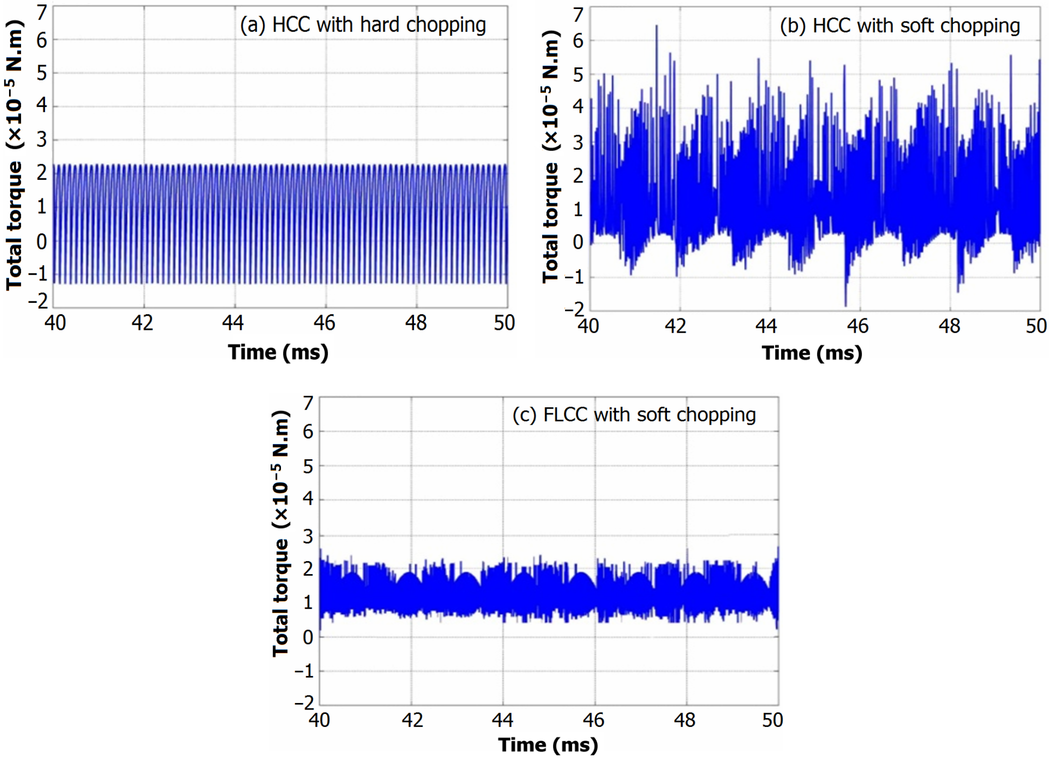

Fig. 9. (Color online) BLDC motor total torque in different chopping modes.

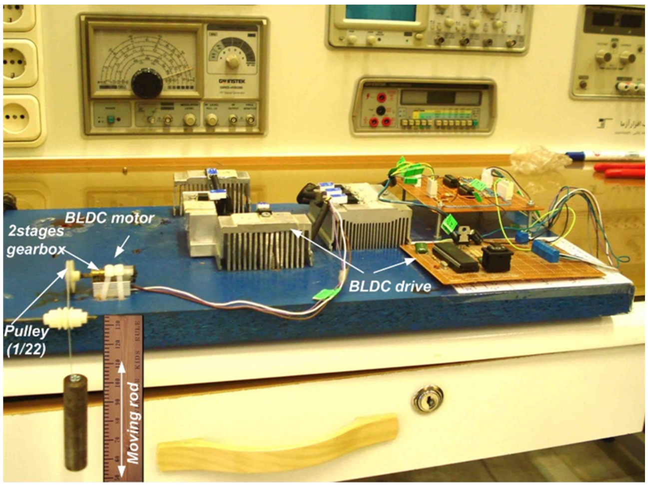

Fig. 10. (Color online) The setup of CRDM.

ping, and FLCC with soft chopping. The results showed the combination of FLCC method with soft chopping as an improved technique for reduction of torque ripple has a good performance. This minimized torque ripple of the BLDC motor drive will directly effect on the movement of the MNSR control rod. In nuclear industrial application, frequent control rod movements for load-following operation induce xenon-oscillation. Therefore, such an FLCC controller together with the soft chopping that can subdue this phenomenon effectively is needed.

[1] Ashabani M, Kashefi Kaviani A, Milimonfared J, *et al.* Minimization of commutation torque ripple in brushless DC motors with optimized input voltage control. International Symposium on Power Electronics, Electrical Drives, Automation and Motion, SPEEDAM, Italy, 2008.

[2] Paul K. US patent 8811562, Control rod drive mechanism for nuclear reactor, 2011.

[3] David P K, Stafford L T, Brian C C. US patent 88634513, System for exchanging a component of a nuclear reactor, 2012.

[4] Divandari M, Shahsavari F, Rezaeimoghadam M, *et al.* A novel control-rod drive mechanism via electromagnetic levitation in MNSR. Nukleonika, 2014, **59**: 73–79. DOI: 10.2478/nuka-2014-0008

[5] Yusuf I, Mati A A. Effects of extended shutdown on the control rod drive mechanism of Nigeria research reactor-1(NIRR-

1). African conference on research reactor utilization and safety, Nigeria, 2010.
[6] International atomic energy agency technology and use of low power research reactors. IAEA-TECDOC-384, 1986.
[7] Divandari M. *et al*. A novel fuzzy dynamic observer for high speed BLDC motor. IEEE XXXIII International Scientific Conference Electronics and Nanotechnology (ELNANO), Ukraine, 2013.